Estimation of electric parameters for thin shielding sheets

Estimation of electric parameters for thin shielding sheets

Toshihide Tosaka
National Institute of Information
and Communications Technology,
Wireless Communications Department
Email: tosaka@nict.go.jp

Isamu Nagano
Graduate School of Natural Science
and Technology, Kanazawa University
nagano@reg.is.t.kanazawa-u.ac.jp

Satoshi Yagitani
Graduate School of Natural Science
and Technology, Kanazawa University
yagitani@reg.is.t.kanazawa-u.ac.jp

***Abstract*— We suggest an estimation method of the electric parameters for thin shielding sheets. In order to evaluate our estimation method, we estimated the electric parameters for the metallic materials which have known electric parameters, and evaluated our method. For the non-magnetic materials, the estimated relative permeability was the same as the nominal values. For the ferromagnetic materials, the estimated relative permeability varied 0% to 30% from the nominal values. For both types of materials, the estimated conductivities were 0% to 9.8% different from the nominal values. Next, we apply our estimation method to shielding sheets, and we can estimate the electric parameters for items such as thin cloths.**

I. INTRODUCTION

With the continuing development of information and electrical technology, the number and kinds of electric devices in our society have increased rapidly. It has been shown that electromagnetic waves leaking from electronic devices may cause incorrect operation of other electronic devices. One method to eliminate the electromagnetic noise which is emitted from electric devices is the use of an electromagnetic shielding sheet. In order to eliminate the electromagnetic noise, the design of the electromagnetic shielding sheet must take into account the electromagnetic field from various noise source points. To do this properly, we must investigate the propagation mechanism of the electromagnetic wave by using numerical analysis. Then it is important to know the electric parameters (ε_r, μ_r, σ), because they are used for calculation of the electromagnetic field.

Methods exist to measure the relative permeability and conductivity of many materials. For most uniform solid materials, the standard way to determine permeability is by generating a B–H curve, and the standard way to measure the conductivity is by using a four-point probe array. But if the materials are thin cloths, such testing would be difficult and the results could be erratic. If the material is thin cloth, such tesging would be difficult and the resutls could be erratic. Because, the surface of this sheet is uneven when observed on a microscopic scale.

In this research, we suggested the new estimation method of the electric parameters. Our method using the electromagnetic wave. To determine the electric parameters of thin shielding materials, we have measured the *SE* using a shielding box and fitted the results to the numerical calculations for a near-field electromagnetic wave [1]. By adjusting the electric parameters

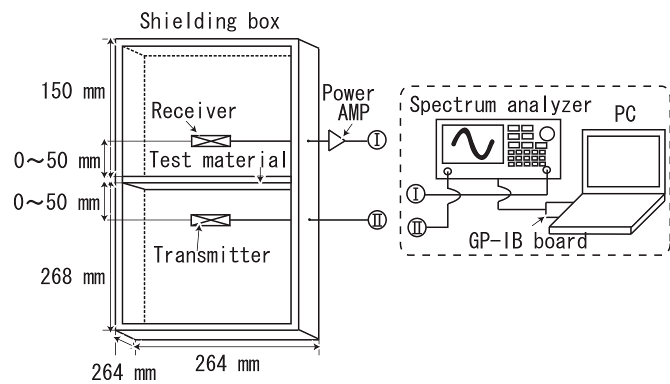

Fig. 1. Estimation system of relative permeability and conductivity

in the calculation until the best fit with the measured values was found, we were able to estimate the electric parameters. For the numerical calculations, we used the Sommerfeld integral [2] that expresses spherical waves by compositions of cylindrical waves.

At first, we estimate the electric parameters for the metallic materials which have know electric parameters. We then compare the values obtained by our method with the nominal values [3], [4]. Finally, we estimate the electric parameters for shielding sheets available in the market today.

II. ESTIMATION SYSTEM

Our estimation system consists of two parts [5] as shown fig. 1. One is the measurement system of *SE*; and the other is the calculation of electric parameters. In this section, we discuussed the measurement method of Shielding Effectiveness (*SE*). *SE* is the rate of interception of magnetic field at the observation point without the testing material (H_0) to that wiht the testing material (H_1):

$$SE = 20log_{10}\frac{H_0}{H_1} \qquad [dB] \qquad (1)$$

We measure the *SE* using a shield box which we developed. This shield box was made from 3 mm thick copper plate. The transmitter and receiver installed in the box. The testing material is placed between the transmitter to the receiver.

If the transmitted magnetic field from the source leaks through the side panels of the shield box, we may not accurately find the *SE* of the testing material. Therefore, the influence of the circumference of the shield box is taken into consideration in the computer simulation. We use a software program named MAFIA [6] which can numerically calculate an electromagnetic field. We found the magnetic field was attenuated more than 20 dB. From the result we find that no waves go outside of the shield box. This means that we should be able to ignore the influence of the side panels and the end panels.

III. Sommerfeld Solution

In calculating an electromagnetic field, we have to consider the locations of the source and the observation point, because the calculations of an electromagnetic field for a near-field point and that for a distant point are quite different. If the distance z from the observation point to a source with wave length λ is $z \gg \lambda/2\pi$, the radiated field is the dominant wave emitted from the source and can be regarded as a plane wave. In this case, the *SE* of the shielding material is not related to the position of the source. But in the shield boxes we used, the distance of the source from the observation point is $z \ll \lambda/2\pi$, and it can not be considered that the radiated field is the wave emitted from source. Thus it is necessary to calculate the electromagnetic field of a near source when calculating *SE*. In this research in consideration of the near source, we used the Sommerfeld integral that expresses spherical waves by a composition of cylindrical waves.

A. Boundary Conditions

When the electric dipole in the Helmholtz equation is replaced with a magnetic dipole, the electromagnetic field is expressed by eq. (2) and eq. (3) by using a magnetic Hertz vector $\mathit{\Pi}_m$. Eq. (4) shows the magnetic Hertz vector $\mathit{\Pi}_m$ related to the magnetic dipole.

$$E = -j\omega\mu\nabla \times \mathit{\Pi}_m \tag{2}$$

$$H = \nabla\nabla \cdot \mathit{\Pi}_m + k^2 \mathit{\Pi}_m \tag{3}$$

$$\mathit{\Pi}_m = \frac{nSI}{4\pi}\frac{e^{-jkR}}{R} i_z \tag{4}$$

Here E is the electric field, H is the magnetic field, j is complex, ω is the angular frequency, μ is the magnetic permeability, k is wave number, n is the number of turns of the source loop current, S is the loop area, I is the loop current, R is the distance from the source, and i_z is the unit vector of z. For numerical analysis, we use the same parameters as used for the measurements.

Then the boundary conditions between the layers i and $i+1$ on the x–y plane can be expressed as in eqs. (5) and (6) by applying the continuity of the H_r and E_θ component to eqs. (2) and (3), where the x–y plane is the horizontal element in Cartesian coordinates.

$$\frac{\partial \mathit{\Pi}_{m,i}}{\partial z} = \frac{\partial \mathit{\Pi}_{m,i+1}}{\partial z} \tag{5}$$

$$\mu_i \mathit{\Pi}_{m,i} = \mu_{i+1} \mathit{\Pi}_{m,i+1} \tag{6}$$

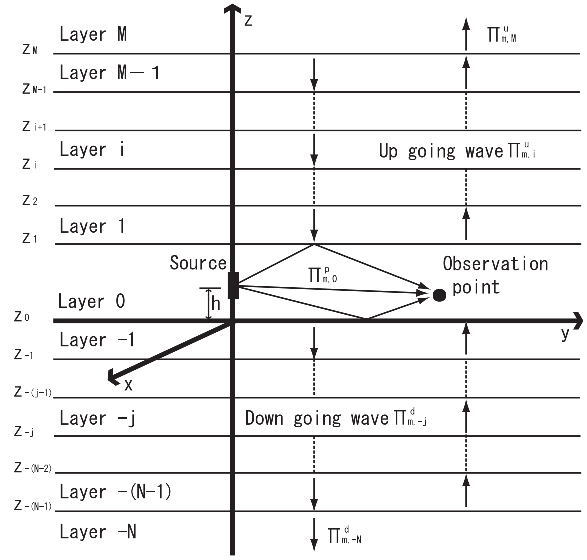

Fig. 2. Multi–layered model.

Here the Hertz vectors for layer *i* and for layer *i*+1 are expressed as $\mathit{\Pi}_{m,i}$ and $\mathit{\Pi}_{m,i+1}$.

B. Electromagnetic analysis by using a multi-layered model

The coordinate system of the multi–layered model which we use to calculate the electromagnetic field is shown in Fig. 2. A magnetic dipole source is assumed at $z = h$ with homogeneous layers above and below the dipole extending to infinity in the horizontal directions. The axial direction of the dipole source is located vertically perpendicular to each layer. The Hertz vector for the up–going wave is expressed as $\mathit{\Pi}^u_{m,i}$, the Hertz vector for the down–going wave is expressed as $\mathit{\Pi}^d_{m,i}$, and the Hertz vector for the direct wave is expressed as $\mathit{\Pi}^p_{m,i}$, where the subscript *i* indicates the layer. The Hertz vector in layer *i* is expressed by eq. (7). By using the Sommerfeld integral representation to express a spherical wave by the synthesis of cylindrical waves, eq. (4) can be transformed into eq. (8) for the up-going waves and into eq. (9) for the down-going waves in layer i.

$$\mathit{\Pi}_{m,i} = \mathit{\Pi}^u_{m,i} + \mathit{\Pi}^d_{m,i} \tag{7}$$

$$\mathit{\Pi}^u_{m,i} = \frac{nSI}{4\pi}\int_0^\infty f^u_{m,i}(\lambda) J_0(\lambda r) e^{-\nu_i(z-z_i)} \lambda d\lambda \tag{8}$$

$$\mathit{\Pi}^d_{m,i} = \frac{nSI}{4\pi}\int_0^\infty f^d_{m,i}(\lambda) J_0(\lambda r) e^{\nu_i(z-z_i)} \lambda d\lambda \tag{9}$$

$$Here \quad \nu_i = \sqrt{\lambda^2 - k_i^2}$$

The integrand elements $f^u_{m,i}$ and $f^d_{m,i}$ are unknown functions of the integration variable λ with the subscripts and superscripts the same as for $\mathit{\Pi}_m$. In appendix 3 we describe how these elements are determined. Here, J_0 is a zero-order Bessel function of the first kind, r is the radial distance in cylindrical coordinates, and z_i is the distance of layer i along the z–axis.

Then we substitute the Hertz vectors (from equation (8) and (9)) into the boundary conditions (5) and (6) in order to solve for the unknown functions $f^u_{m,i}$, $f^d_{m,i}$. This expresses the results as a known 2 × 2 matrix including a_{11}, a_{12}, a_{21}, a_{22} as shown eq. (10).

$$\begin{aligned}\begin{pmatrix} f^u_{m,i} \\ f^d_{m,i} \end{pmatrix} &= \frac{1}{2\mu_i\nu_i}\begin{pmatrix} (\mu_i\nu_{i+1}+\mu_{i+1}\nu_i)e^{\nu_i(z_i-z_{i-1})} & (-\mu_i\nu_{i+1}+\mu_{i+1}\nu_i)e^{\nu_i(z_i-z_{i-1})} \\ (-\mu_i\nu_{i+1}+\mu_{i+1}\nu_i)e^{-\nu_i(z_i-z_{i-1})} & (\mu_i\nu_{i+1}+\mu_{i+1}\nu_i)e^{-\nu_i(z_i-z_{i-1})} \end{pmatrix}\begin{pmatrix} f^u_{m,i+1} \\ f^d_{m,i+1} \end{pmatrix} \\ &\equiv \begin{pmatrix} a_{11} & a_{12} \\ a_{21} & a_{22} \end{pmatrix}\begin{pmatrix} f^u_{m,i+1} \\ f^d_{m,i+1} \end{pmatrix} \end{aligned} \quad (10)$$

Then expanding from layer 0 to layer M, eq. (10) can be transformed to eq. (11).

$$\begin{pmatrix} f^u_{m,0} \\ f^d_{m,0} \end{pmatrix} = \prod_{i=0}^{M-1}\begin{pmatrix} A_{11} & A_{12} \\ A_{21} & A_{22} \end{pmatrix}\begin{pmatrix} f^u_{m,M} \\ 0 \end{pmatrix} - \frac{1}{\nu_0}\begin{pmatrix} e^{\nu_0 h} \\ 0 \end{pmatrix} \quad (11)$$

Here, A_{11}, A_{12}, A_{21}, A_{22} are components of the known matrix, and h is the distance from the origin.

Similarly, expanding from layer 0 to layer -N using boundary conditions, we calculate the Hertz vectors for layer 0 to -N of the matrix below the source. We are able to find the unknown parameters by solving the equality for layer 0 for the two cases. Using these derived unknown matrices, we can calculate the electromagnetic field in arbitrary layer i.

We used the Sommerfeld integral which expresses a spherical wave by composition of cylindrical waves, and for the numerical calculation we used the trapezoidal rule on the real axis. Since the integral converges as the numerical calculation proceeds, the processing is terminated as soon as the integrated value does not change. We find using this method to be very effective, because results of comparing e^{-jkR}/R with the Sommerfeld integral are very close up to the eighth decimal place. Therefore, we are able to validate our method.

IV. Estimation method

In order to estimate the electric parameters, we first measured *SE* with the shield box. Then from these *SE*, we estimate the electric parameters of metallic materials. The *SE* calculations are most influenced by the electric parameters. *SE* has different characteristics as a function of frequency for different types of materials. Fig. 3 shows *SE* of metal materials. In the case of non-magnetic materials (Al, Pb, Cu), the measurement value and the calculation value that used the nominal value of the electric parameters are very close. In these cases, we can estimate the electric parameters with high accuracy. But for ferromagnetic materials (Fe, Ni), as the frequency becomes high, the calculated *SE* becomes much larger than the measured *SE*.

Therefore, we then calculated *SE* by taking the frequency characteristics into account. Fig. 4 shows *SE* when the

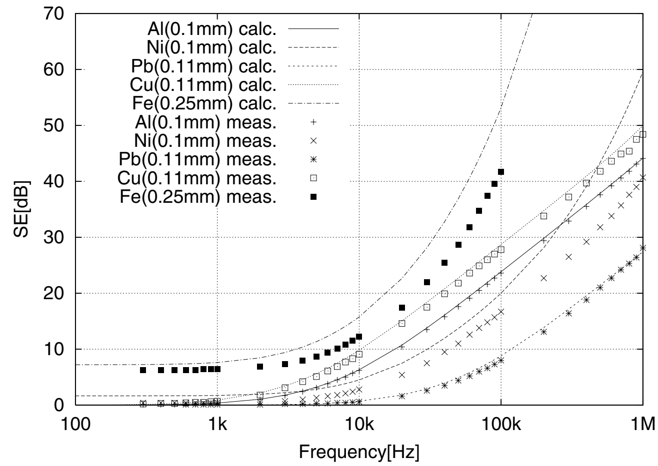

Fig. 3. *SE* of metallic materials

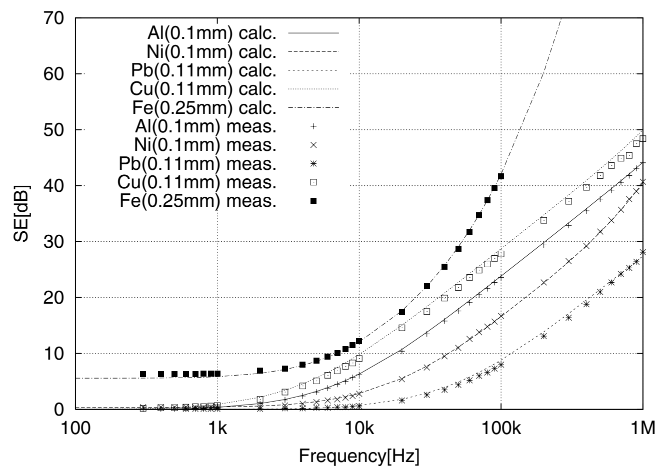

Fig. 4. *SE* of metallic materials after consideration of frequency characteristics

frequency characteristics of the relative permeability were considered. From fig. 3 in the low frequency region where the calculated and measured *SE* values were close, we used the estimation method to determine the conductivity which does not change with frequency. Using the conductivity as a constant, we then varied the relative permeability to find the minimum value of the difference. In this computation, we used the least squares method.

In this way, by changing the relative permeability parameter, we can estimate the frequency characteristics of the relative permeability as shown in Fig. 5. Since most of the data of relative permeability available in reference books are for DC, we have to determine for ourselves the nominal values for the AC case. In order to determine the nominal values for the AC case, we determined the relative permeability as a function of frequency by using B–H curves generators. When this was completed, we evaluated our estimation method.

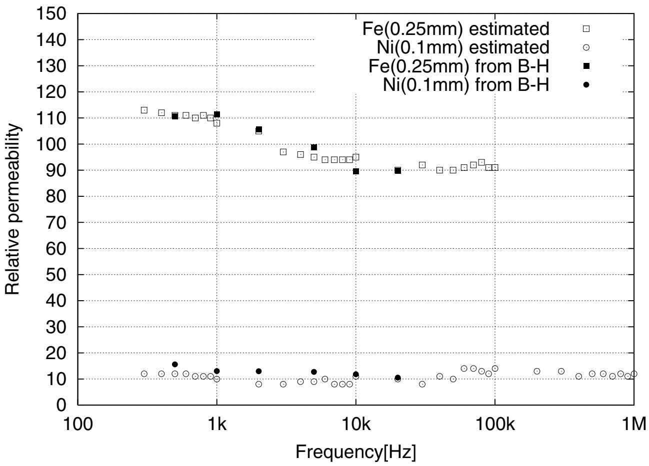

Fig. 5. The frequency characteristics of the relative permeability

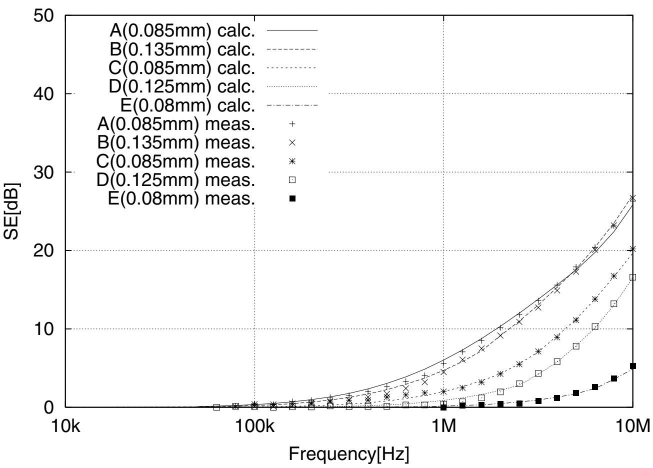

Fig. 6. *SE* of electromagnetic shielding sheets

V. Results of Estimation

Table I shows the relative permeability and conductivity of metallic materials. The calculated conductivity was the same as the nominal value for Pb, 1.9% greater for Cu, and 3.3% greater for Al. For the ferromagnetic materials, the calculated value was 4.1% higher for Ni and 9.8% higher for Fe. For comparison, measurement of conductivity using the four point probe method had a typical error rate of about 20%. Thus, we find that our method is better than the existing method. The nominal values for the relative permeability of the ferromagnetic materials are close to the values derived with our B–H curve testing as shown in Fig. 5. For Fe, the nominal and calculated values ranged from the same to 3% difference. For Ni, they ranged from the same to 33% difference from the nominal values.

VI. Estimation for Thin Shielding Sheets

We developed an estimation method for electric parameters for non-magnetic materials and ferromagnetic materials. Next we applied it to shielding sheets that are commercially available, and estimate the electric parameters for these materials. The shielding sheets are compounded materials and are made of polyester fibers which are plated with metallic materials such as copper or nickel. Therefore, electric parameters are unknown for them or difficult to measure. For example, the sensor connections to the testing materials such as required for the four-point prove array method might find the needles on, among, or through the fibers and the results would be erratic.

We used the five materials listed in table II. Table II lists the materials and their plating metals. The parentheses enclose the thickness of the materials. The distance from the transmitter to the receiver is 20 mm. Fig. 6 shows the *SE* of the shielding sheets. The symbols are the measured values of *SE* and the lines are the best fitted solutions for the estimation. From these lines, we determine the electric parameters. The estimation method for metallic materials is different for non-magnetic materials and ferromagnetic materials. For the case of the shielding sheets, we consider the plated materials too. If the plated material contained ferromagnetic materials, we consider the frequency characteristics of the relative permeability. For the case of ferromagnetic materials, we first determine the conductivity in the low frequency range until the difference between the calculated value and the measured value of the *SE* exceeds 3 dB.

For the situation of thin shielding sheets, we do not know the materials' electric parameters. But the point of frequency where the difference between the calculated values and the measured values becomes greater than 3 dB relates to the thickness. Then, we determine the conductivity at low frequency and estimate the relative permeability considering frequency characteristics using the derived conductivity. For the case of materials that are plated with ferromagnetic materials, the relative permeability is very low. Therefore, there are no frequency characteristics for relative permeability less than the 10 MHz frequency range. Table II shows the results of estimation for shielding sheets. Then, we can estimate the electric parameters for materials which have unknown electric parameters such as thin shielding sheets.

VII. Conclusion

We measured *SE* using a shield box. Since near-field and far-field calculation methods are different, we had to consider the distance from the source to the observation point. For our measurements, the distances from the dipole source to the observation point are smaller than a wave length. We calculated the electromagnetic field at the observation point by using the Sommerfeld integral that expresses spherical waves as compositions of cylindrical waves.

Measurement values of the non-magnetic materials materials of *SE* are very close to the calculated *SE* values using nominal electric parameters, and we were able to estimate the electric parameters easily. But in the case of ferromagnetic materials, the measurement values and the calculated values differ as the frequency increases. When we considered the frequency characteristics of the electric parameters, changing

TABLE I

NOMINAL ELECTRIC PARAMETER VALUES COMPARED TO ESTIMATED VALUES

Materials (thickness)	μ_r [nom. / cal.]	σ [S / m] [nom. / cal.]
Al (0.1 mm)	1.0 / 1.0	3.63×10^7 / 3.51×10^7
Cu (0.11 mm)	1.0 / 1.0	5.80×10^7 / 5.69×10^7
Pb (0.11 mm)	1.0 / 1.0	0.50×10^7 / 0.50×10^7
Fe (0.25 mm)	111.0 / 108.0	1.02×10^7 / 0.92×10^7
Ni (0.1 mm)	13.0 / 10.0	1.45×10^7 / 1.39×10^7

TABLE II

RESULTS OF ESTIMATION FOR THIN SHIELDING SHEETS

Material (thickness)	μ_r	σ [S / m]
A (0.085mm)	1.0	4.38×10^5
B (0.135mm)	2.0	2.55×10^5
C (0.08mm)	1.0	2.17×10^5
D (0.125mm)	1.0	8.80×10^4
E (0.085mm)	1.0	3.10×10^5

the parameters allowed us to determine the relative permeability and conductivity as a function of frequency. Finally, we applied it thin sheilding sheets.

Using our method, we can estimate the electric parameters not only for non-magnetic materials but also for ferromagnetic materials. This will be very useful for the simulation of electromagnetic fields. And we hope that the present experimental studies help simulate an electromagnetic field's effect on a human's body and improve measures for EMC.

REFERENCES

[1] T. Tosaka, I. Nagano, S. Yagitani, and Y. Yoshimura, "Determining the relative permeability and conductivity of thin materials," *IEEE Trans. Electromagn. Compat.*, Paper in Press.

[2] A. Sommerfeld, "Electrodynamics, translated by Edward G. Rambe," *Academic Press, New York*, 1964.

[3] F. M. Tesche, M. V. Ianoz, T. Karlsson, "EMC analysis methods and computational models," *A Wiley-Interscience*, pp. 550-552, 1997.

[4] W. H. Jr Hayt "Engineering Electromagnetics," *McGraw-Hill Book co*, 1981.

[5] T. Tosaka, I. Nagano, S. Yagitani, and Y. Yoshimura, "Development of estimation system of relative permeability and conductivity of thin materials," *IEICEJ Trans. Commun., Vol. J87–B, No. 11*, pp. 1943–1950, Nov. 2004.

[6] "MAFIA Release 4.00," *Gesellschaft für Computer–Simulationstechnik m. b. H.*, 1997